



PCCP

Failure of Molecular Dynamics to Provide Appropriate Structures for Quantum Mechanical Description of the Aqueous Chloride Ion Charge-Transfer-to-Solvent Ultraviolet Spectrum

Journal:	<i>Physical Chemistry Chemical Physics</i>
Manuscript ID	CP-ART-03-2021-000930.R1
Article Type:	Paper
Date Submitted by the Author:	28-Mar-2021
Complete List of Authors:	Chipman, Daniel; University of Notre Dame, Radiation Laboratory Marin, Timothy; Benedictine University, Physical Sciences Janik, Ireneusz; University of Notre Dame, Radiation Laboratory Bartels, D; University of Notre Dame, Notre Dame Radiation Laboratory

SCHOLARONE™
Manuscripts

Cite this: DOI: 00.0000/xxxxxxxxxx

Failure of Molecular Dynamics to Provide Appropriate Structures for Quantum Mechanical Description of the Aqueous Chloride Ion Charge-Transfer-to-Solvent Ultra-violet Spectrum

Timothy W. Marin,^a Ireneusz Janik,^b David M. Bartels,^b and Daniel M. Chipman^{*b}

Received Date

Accepted Date

DOI: 00.0000/xxxxxxxxxx

The lowest band in the charge-transfer-to-solvent ultraviolet absorption spectrum of aqueous chloride ion is studied by experiment and computation. Interestingly, the experiments indicate that at concentrations up to at least 0.25 M, where calculations indicate ion pairing to be significant, there is no notable effect of ionic strength on the spectrum. The experimental spectra are fitted to aid comparison with computations. Classical molecular dynamic simulations are carried out on dilute aqueous Cl^- , Na^+ , and NaCl , producing radial distribution functions in reasonable agreement with experiment and, for NaCl , clear evidence of ion pairing. Clusters are extracted from the simulations for quantum mechanical excited state calculations. Accurate *ab initio* coupled-cluster benchmark calculations on a small number of representative clusters are carried out and used to identify and validate an efficient protocol based on time-dependent density functional theory. The latter is used to carry out quantum mechanical calculations on thousands of clusters. The resulting computed spectrum is in excellent agreement with experiment for the peak position, with little influence from ion pairing, but is in qualitative disagreement on the width, being only about half as wide. It is concluded that simulation by classical molecular dynamics fails to provide an adequate variety of structures to explain the experimental CTTS spectrum of aqueous Cl^- .

INTRODUCTION

Ultraviolet (UV) excited states of aqueous chloride ion, as well as other halides and many additional anions, are known as charge-transfer-to-solvent (CTTS) states.^{1–3} All excited electronic states of Cl^- are unbound in the gas phase. However, the lowest UV band in the aqueous spectrum that peaks at ~ 7.1 eV^{4–6} arises from bound excited states, which exist by virtue of the interaction of Cl^- with surrounding water. These states are of particular interest inasmuch as they allow for probing the local solvent environment and because their partial delocalization onto neighboring water molecules promotes dynamical electron detachment to ultimately form hydrated electrons^{2,3} such as are ubiquitous in aqueous radiation chemistry.^{7–9}

Kim *et al.* have reported quantum mechanical (QM) results for the lowest CTTS states in small gas phase clusters $\text{Cl}^-(\text{H}_2\text{O})_n$ having $n=1-4$ ^{10,11} and $n=5-6$,¹² and have further used *ab initio* molecular dynamics (AIMD) to follow the time evolution of a cluster having $n=3$.¹³ Sheu and Liu have also reported QM CTTS

results for gas phase clusters having $n=2-6$.^{14,15}

Other computational studies have used AIMD with periodic boundary conditions to simulate the bulk water phase in order to study CTTS of aqueous Cl^- . Borigs and Staib^{16–20} treated Cl^- as one QM valence electron outside a pseudopotential core, with water molecules treated by molecular mechanics (MM), finding that the lowest vertical excited states qualitatively correspond to $3p$ -like to $4s$ -like transitions of Cl^- , and subsequently followed the dynamical detachment of the excited electron. Costa Cabral *et al.*²¹ have carried out AIMD using a full quantum treatment of Cl^- coordinated to 0-6 explicit water molecules together with representation of many additional water molecules as point charges. Clusters extracted as snapshots from the simulation were subjected to QM calculations, finding that the excited electron delocalizes over a small number of water molecules in the first solvation shell and in a cavity close to some hydrogen atoms.

The present work is the first attempt to computationally interpret the shape, particularly the width, as well as the position of the lowest band in the experimental CTTS UV spectrum of Cl^- in bulk water. It uses a strategy analogous to one that was carried out to study the CTTS spectrum of aqueous iodide I^- ²² in which classical molecular dynamics (MD) is employed to obtain

^a Department of Physical Sciences, Benedictine University, 5700 College Rd, Lisle, IL 60532

^b Radiation Laboratory, University of Notre Dame, Notre Dame, IN 46556-5674.

structures for subsequent QM calculations.

The next section describes a new experimental spectrum and empirical fits to the observed spectra for use in evaluating the computations. Following that is a section on classical MD simulations of aqueous Cl^- , Na^+ , and NaCl to obtain representative structures for QM analysis. Then comes a section describing QM calculations on vertical excited states of Cl^- in which the environment is mimicked by using clusters extracted from the MD simulations along with dielectric continuum surrounding the explicit water molecules. The work ends with a concluding discussion.

FIT TO THE EXPERIMENTAL CHLORIDE ION UV SPECTRUM

There are several experimental reports of the Cl^- UV spectrum in dilute aqueous KCl solution.^{4–6} The latter work⁶ provides the most recent and detailed spectra, ranging from near ambient conditions to highly elevated temperatures, but only the near ambient spectrum will be considered here. The experimental procedure has been previously described in full detail.⁶ Data were collected at two salt concentrations, 0.025 M and 0.250 M, although only the 0.025 M spectrum was presented previously. The spectra obtained at both concentrations are shown in Fig. 1. Data below 5.8 eV are omitted since in each case the absorption coefficient has only very small background values there. The chlorine atom spin-orbit splitting of 0.109 eV²³ is too small to be resolved in the extant experiments. While the spectra at the two concentrations are very similar on the near low energy sides of the peaks at $\lesssim 7.10$ eV, there are notable differences elsewhere.

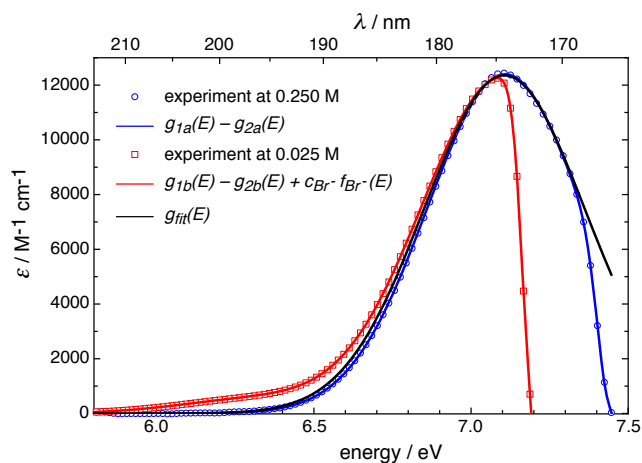


Fig. 1 UV spectrum of aqueous Cl^- from experiments and empirical fits.

Both cases have a cutoff at higher energies, beginning at ~ 7.35 eV for the 0.250 M case and at ~ 7.10 eV for the 0.025 M case. These high energy cutoffs are due in part to masking by the onset of the rising edge of the water solvent UV absorption band. This absorption is more significant in the 0.025 M case because of the ten times longer path length used in that experiment, increasing the magnitude of the water absorption tenfold and therefore shifting the cutoff to lower energy. Also, above these cutoff energy thresholds, multiple experimental artifacts arising from diminishingly small levels of light transmission compound to give rise to a

Table 1 Parameters of fits to the raw experimental UV spectra of aqueous chloride ion. The Br^- correction term has optimum coefficient $c_{\text{Br}^-} = 0.00532$

	ϵ_{\max} ($\text{M}^{-1} \text{cm}^{-1}$)	E_0 (eV)	σ (eV)
$g_{1a}(E)$	12400	7.108	0.247
$g_{2a}(E)$	4900	7.442	0.039
$g_{1b}(E)$	12000	7.104	0.263
$g_{2b}(E)$	11400	7.198	0.033
$g_{\text{fit}}(E)$	12200	7.106	0.255

cutoff that is not vertical in nature, nor necessarily consistent in slope between the two samples. Corrections made at the two different concentrations for these issues are therefore not expected to peak at the same position. The shape of this cutoff edge can be addressed in an empirical manner, as shown below.

Compared to the 0.250 M spectrum, the 0.025 M spectrum has a distinct shoulder at lower energies centered at ~ 6.3 eV. This is believed to be due to contamination by a small amount of KBr, whose region of peak absorbance covers the shoulder region.⁶ The sample cell had been used for a KBr experiment just prior to the KCl experiment quoted here, and the KBr was evidently not completely flushed away.

These differences between the two spectra can be reconciled through empirical fitting. The fitting procedure uses gaussians having the generic form

$$g(E) = \epsilon_{\max} e^{-(E-E_0)^2/2\sigma^2}.$$

The full width at half maximum (FWHM) of such a gaussian is $2\sqrt{2\log 2}\sigma \approx 2.355\sigma$.

The extinction coefficient observed for the 0.250 M spectrum, labelled as “a”, can be fit with two terms according to

$$\epsilon_a(E) = g_{1a}(E) - g_{2a}(E).$$

The gaussian $g_{1a}(E)$ is mostly sensitive to the region near the peak. Subtracted from it is a gaussian $g_{2a}(E)$ that describes the high energy cutoff due to interferences from water absorption and experimental artifacts. This fit, shown in Fig.1, provides an excellent representation of the raw experimental data. The best fit parameters are given in Table 1

The extinction coefficient observed for the 0.025 M spectrum, labelled as “b”, can be fit with three terms according to

$$\epsilon_b(E) = g_{1b}(E) - g_{2b}(E) + c_{\text{Br}^-} f_{\text{Br}^-}(E).$$

The gaussians $g_{1b}(E)$ and $g_{2b}(E)$ have interpretations analogous to those just noted above. Added to them is a multiple of the known 2-gaussian fit,⁶ labelled here as $f_{\text{Br}^-}(E)$, of the aqueous Br^- spectrum that describes the low energy shoulder that is believed due to absorption by a small amount of Br^- contaminant. This fit, shown in Fig. 1, provides an excellent representation of the raw experimental data. The best fit parameters are given in Table 1.

Assuming that the high energy cutoffs in both spectra and the low energy shoulder in the 0.025 M spectrum are indeed cor-

rectly interpreted as interferences, the only parts of the two fitted spectra actually due to Cl^- are the gaussians $g_{1a}(E)$ and $g_{1b}(E)$. Consistent with this understanding, these two gaussians agree to within the expected experimental error. The best estimate of the actual Cl^- spectrum is then taken to be a single gaussian $g_{fit}(E)$ having parameters averaged over those of $g_{1a}(E)$ and $g_{1b}(E)$, giving the values included in Table 1. This fit has FWHM of 0.601 eV. It is included in Fig. 1, where it differs significantly from the experimental 0.250 M spectrum only at energies higher than ~ 7.35 eV where the experimental values are subjected to interference.

It is concluded that the UV spectrum of aqueous Cl^- at concentrations of 0.025 M and 0.250 M can be accurately described as the single gaussian $g_{fit}(E)$, at least up to energies of ~ 7.35 eV and likely somewhat higher. This is the target that the computations presented in the remainder of this study attempt to interpret.

It is surprising that the spectra are essentially identical at both concentrations examined, showing that, at least up to concentrations of 0.25 M, ionic strength has no notable effect on the spectrum. This implies either that ion pairing does not significantly occur at these concentrations or that if it does occur its various effects conspire together to accidentally cancel its influence on the spectrum. The latter would imply that in some overall average manner the effect of ion pairing is about the same on the ground state energy as on the excited state energies, causing a coincidental negation of its influence on the transition energies.

MOLECULAR DYNAMICS SIMULATIONS

MD Methods

Classical molecular dynamic simulations were carried out with the Tinker 8.6.1 program package^{24,25} using the AMOEBA15 force field for water²⁶ together with parameters for Cl^- and Na^+ deemed in that work to be consistent with it. This flexible and polarizable multipole force field has been shown to provide an accurate description of many properties of gas phase water clusters and aqueous water over a wide temperature range, and also of the gas phase water- Cl^- and water- Na^+ dimer binding energies and of their aqueous ion solvation free energies.²⁶

While the experiments for comparison were done with KCl solutions, NaCl has been used here instead because of the availability of suitable AMOEBA15 parameters for Na^+ and the expectation that the counterion identity should be of little consequence for the Cl^- spectrum in dilute solution. Indeed, experimental evidence indicates that aqueous chloride ion has local coordination that is quite insensitive to counterion, ionic strength, or moderate changes in temperature and pressure.²⁷

Temperature was held nearly constant at 298K through velocity scaling regulated by the Berendsen weak-coupling thermostat.²⁸ This strictly gives an ensemble intermediate between canonical and microcanonical,²⁹ which with the default coupling time constant of 0.1 ps used in the calculations reported herein approaches closely to the weak coupling limit of the canonical ensemble. Periodic boundary conditions were invoked, using particle-mesh Ewald summation of order 8 for electrostatic interactions with a cutoff radius of 9 Å. The van der Waals interactions beyond 12 Å were tapered to zero with a 1.2 Å switching function. The

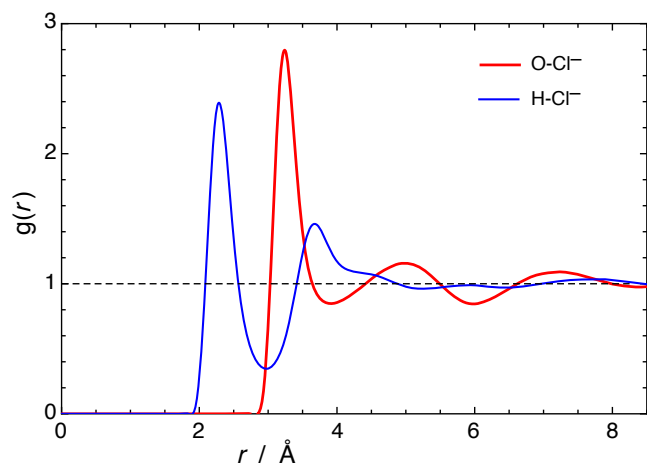


Fig. 2 Radial distribution functions calculated for O- Cl^- and H- Cl^- in water.

Table 2 Comparison of the first RDF maxima in Å and the Cl^- coordination number from neutron diffraction (ND), extended X-ray diffraction absorption fine structure (EXAFS), and X-ray diffraction (XRD) on dilute NaCl to the present molecular dynamics (MD) simulations on dilute Cl^-

Method	O- Cl^-	H- Cl^-	coordination
ND ⁸⁰	3.16±0.11	2.19±0.16	6.9±1.0
EXAFS ⁸¹	3.1±0.10	2.18±0.10	7
ND,XRD ⁸²	3.22±0.02	2.29±0.01	5.9±0.9
MD	3.25	2.28	7.0

equations of motion were integrated with a modified Beeman algorithm^{30,31} using time steps of 1.0 fs. Induced dipoles were converged to 10^{-4} D rms.

In all the simulations snapshots for analysis were saved at 1 ps intervals. Radial distribution functions (RDFs) $g(r)$ were obtained from histograms having bins 0.10 Å wide fitted for display by spline smoothing.

MD Simulations on Cl^- in Water

Starting points for the Cl^- simulations were initialized from a previously equilibrated cubic box containing 216 water molecules and having edges of 18.643 Å to reproduce the experimental density at 298K. One randomly selected water molecule was replaced with a Cl^- to produce an ion concentration of 0.256 M. This starting configuration was first equilibrated for 50 ps and then propagated in ten separate trajectories having different initialization seeds. Each trajectory was run for 10 ns, producing a combined total of 100 ns of Cl^- data.

The O- Cl^- and H- Cl^- RDFs obtained from the Cl^- simulations are shown in Fig. 2. Similar results have been reported in many other computational studies using various methods, including classical MD,^{32–57} Monte Carlo,^{38,58–62} integral equation techniques,^{63–69} AIMD,^{70–78} and QM/MM⁷⁹ approaches.

The positions of the first RDF maxima and the Cl^- coordination number, determined by integration of the O- Cl^- RDF out to the first minimum that occurs at 3.92 Å, are given in Table 2 along with experimental results obtained from dilute (<0.7 M) NaCl so-

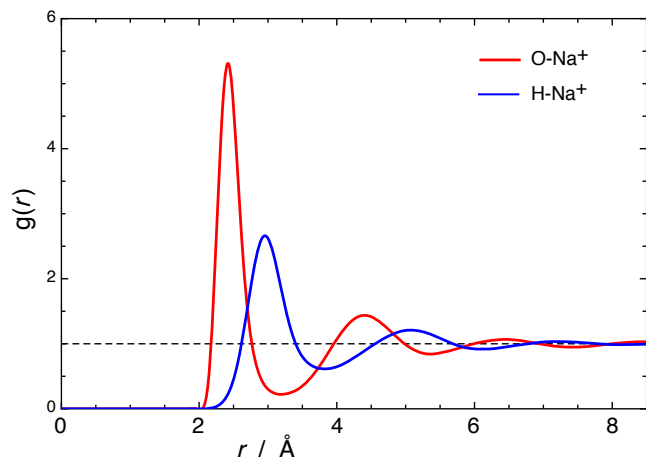


Fig. 3 Radial distribution functions calculated for O-Na⁺ and H-Na⁺ in water.

lutions in the literature. In addition, the second RDF maxima can be estimated from Fig. 6 in a neutron diffraction experiment⁸⁰ to be at ~ 5.1 Å for O-Cl⁻ and ~ 3.5 Å for H-Cl⁻ compared to 4.98 Å and 3.67 Å, respectively, from the MD simulations. The present results are seen to closely agree with those from the various experiments. For the record, it is noted that integration of the computed O-Cl⁻ RDF from the first to the second minimum that is located at 6.00 Å gives a coordination number of 22 water oxygens in the second solvation shell, and that the first minimum of the H-Cl⁻ RDF occurs at 2.97 Å.

MD Simulations on Na⁺ in Water

MD simulations on Na⁺ were carried out entirely analogously to those already described for Cl⁻. Ten separate trajectories having different initialization seeds were each propagated for 10 ns, producing a combined total of 100 ns of Na⁺ data.

The O-Na⁺ and H-Na⁺ RDFs obtained from the Na⁺ simulations are shown in Fig. 3. Similar results have been reported in many other computational studies using various methods, including classical MD,^{32–35,37–41,43–45,47–49,51,52,54,56,57,83–85} Monte Carlo,^{58–61} integral equation techniques,^{63–69,86} and AIMD,^{71,72,74,76,77}

The positions of the first O-Na⁺ and H-Na⁺ maxima and the Na⁺ coordination number, determined by integration of the O-Na⁺ RDF out to the first minimum that occurs at 3.19 Å, are given in Table 3 along with experimental results obtained from dilute (<0.7 M) NaCl solutions in the literature. The present results are again seen to closely agree with those from the various experiments. Integration from the first to the second minimum that is located at 5.35 Å gives a coordination number of 16 water oxygens in the second solvation shell. For the record, it is noted that the second maximum in the computed O-Na⁺ RDF lies at 4.40 Å, and the first minimum and second maximum in the H-Na⁺ RDF lie at 3.82 and 5.07 Å, respectively.

Table 3 Comparison of the first RDF maxima in Å and the Na⁺ coordination number from neutron diffraction (ND) and X-ray diffraction (XRD) on dilute NaCl to the present molecular dynamics (MD) simulations on dilute Na⁺

Method	O-Na ⁺	H-Na ⁺	coordination
ND ⁸⁰	2.34±0.14	2.97±0.12	5.3±0.8
ND,XRD ⁸²	2.37±0.08	-	5.1±0.7
MD	2.42	2.95	5.6

MD Simulations on NaCl in Water

Starting points for the NaCl simulations were initialized by replacing one randomly selected water molecule from the 216 water box described above with a Cl⁻ ion and a second water molecule with a Na⁺ ion to produce a salt concentration of 0.256 M. Three different possibilities for the initial Na⁺-Cl⁻ distance were considered, at ~ 3 Å, ~ 5 Å, and ~ 8 Å. Each of these starting configurations was equilibrated for 50 ps with the constraint of holding the Na⁺-Cl⁻ distance nearly constant, and then propagated in ten separate trajectories having different initialization seeds. Each trajectory was run for 10 ns, producing 100 ns of data from each starting configuration for a combined total of 300 ns of data.

The Na⁺-Cl⁻ RDFs obtained from the three separate 100 ns sets of data resulting from different starting separations give very similar, albeit “noisier”, RDFs as that shown in Fig. 4 from the entire combined data set, showing that in each case sufficient simulation time was allowed for the ions to fully sample the entire range of available Na⁺-Cl⁻ distances. The RDFs show clear indications of Na⁺-Cl⁻ ion pairing.

The status of ion pairing in dilute aqueous NaCl is open to question. A critical review of available experimental evidence obtained from conductivity, potentiometry, activity and osmotic coefficients, solubility, and various spectroscopies including dielectric and ultrasonic relaxation, UV-vis, infrared, Raman, and nuclear magnetic resonance has concluded that there is lingering doubt about the reality of ion pairing for low charge electrolytes in high permittivity solvents such as water.⁸⁷ Contrary to that is the isolated claim based on evidence from infrared spectroscopy that, rather than all ions being individually well solvated, in fact all ions in NaCl solution exist as bonded ion pairs even down to concentrations as low as 0.002 M.⁸⁸ Ion pairing in dilute aqueous NaCl solution has been consistently found in a variety of computational approaches, including classical MD,^{40,43,44,47,48,54,56,83,89–112} integral equation techniques,^{63–67,69,86,113–118} continuum electrostatics models,^{119,120} Langevin dynamics,^{121–124} Monte Carlo,^{60,125,126} and AIMD^{104,127} simulations.

For purposes of discussion snapshots having Na⁺-Cl⁻ distances up to the first minimum in the associated RDF at 3.74 Å will be categorized as being contact ion pairs (CIP), those between the first and second minimum at 6.04 Å as solvent-shared ion pairs (SIP), those between the second and third minimum at 8.05 Å as solvent-separated ion pairs (2SIP), and those beyond the third minimum as being effectively unpaired and therefore free from ion-ion interaction (Free). That should appropriately classify the large majority of structures, although it is recognized that there

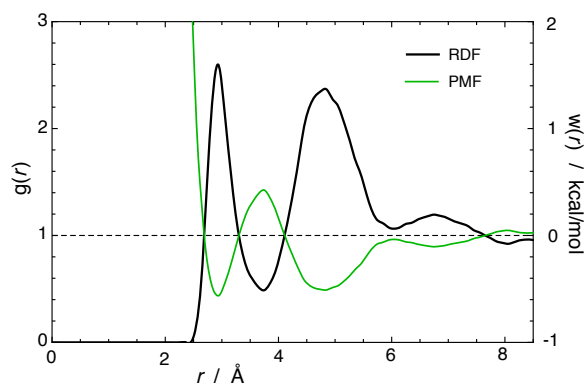


Fig. 4 Radial distribution function (black, left axis) and potential of mean force (green, right axis) for $\text{Na}^+\text{-Cl}^-$ in water.

are other reasonable categorization schemes, and that such would likely differ for some of the snapshots, particularly for those near the cutoff minima. It should be pointed out that characterization of the outermost minimum is likely less reliable than the others because of edge effects due to the finite size of the simulation box.

Maxima of the present calculated $\text{Na}^+\text{-Cl}^-$ RDF occur in the CIP, SIP, and 2SIP regions at 2.93, 4.8, and 6.8 Å, respectively. X-ray diffraction measurements down to 0.5 M NaCl fitted subject to constraints based on MD simulations find the first two peaks in the $\text{Na}^+\text{-Cl}^-$ RDF to be at 2.80 ± 0.01 Å and 5.10 ± 0.01 Å.⁴⁷ Neutron diffraction experiments down to 0.67 M NaCl massaged by an empirical potential structure refinement find the first two peaks in the $\text{Na}^+\text{-Cl}^-$ RDF to be at ~ 2.75 Å and ~ 5.1 Å.⁸⁰ These values are in fair agreement with those calculated here for CIP and SIP. Minima of the RDF occur at 3.74, 6.04, and 8.05 Å such that the CIP region has 2.8% of the total salt population, the SIP region 17%, the 2SIP region $\sim 21\%$, and the remaining Free region $\sim 59\%$.

The potential of mean force (PMF) $w(r)$ between ions, as obtained from the $\text{Na}^+\text{-Cl}^-$ RDF by means of the relation¹²⁸ $w(r) = -k_B T \log g(r)$ is included in Fig. 4. Positions of minima and maxima of the $\text{Na}^+\text{-Cl}^-$ PMF mirror those of the RDF. Working from shorter to larger distances, PMF energies at the minima are -0.56 , -0.51 , and -0.11 kcal/mol, while energies at the maxima are 0.43 , -0.04 , and 0.05 kcal/mol. These produce dissociation and association barriers in kcal/mol of 0.99 for CIP \rightarrow SIP and 0.94 for CIP \leftarrow SIP. Compared to thermal energy $k_B T$ of 0.59 kcal/mol, this indicates partial hindering of passage back and forth between these regions. Dissociation and association barriers in kcal/mol are 0.47 for SIP \rightarrow 2SIP and 0.07 for SIP \leftarrow 2SIP, and 0.15 for 2SIP \rightarrow Free and 0.05 for 2SIP \leftarrow Free, implying that facile movement is allowed among these outer regions. Similar PMF results have been obtained through more direct methods in a number of the studies referenced above.

QUANTUM MECHANICAL CALCULATIONS

Overall, it is concluded that MD simulations with the AMOEBA15 force field give reasonable agreement with experiment for a disparate assortment of Cl^- properties in dilute aqueous solution, in-

cluding the solvation energy, coordination number, the O- Cl^- and H- Cl^- RDFs, and likely also for the $\text{Na}^+\text{-Cl}^-$ RDF and PMF. Snapshots from the MD simulations can therefore plausibly be used to provide structures for subsequent QM treatment. Selected snapshots were always separated by at least 20 ps to minimize the possibility of obtaining correlated structures. The QChem5 program package¹²⁹ was used for all the QM calculations.

QM Benchmarks

Twenty snapshots from the MD simulations of aqueous Cl^- were chosen for benchmark treatment to enable determination of a satisfactory efficient QM protocol. Clusters containing Cl^- and all its first-shell water molecules were extracted from the selected snapshots, where first-shell water molecules were taken as all those having O- Cl^- distances up to the first minimum of the corresponding RDF. The twenty clusters were chosen randomly, except for the provision of having five representatives each of 5-, 6-, 7-, and 8-coordination in the first solvation shell.

The selected clusters were treated with benchmark calculations using the EOM-CCSD method^{130,131} with the aug-cc-pVDZ basis set,^{132,133} together with a dielectric continuum treatment¹³⁴ of the region outside the explicitly treated atoms. The dielectric continuum treatment is a modification of the COSMO method¹³⁵ that is variously known as GCOSMO¹³⁶ or CPCM.¹³⁷ It is closely related to the currently used version of the IEFPCM method,¹³⁸ which is formally equivalent to the SS(V)PE method^{139,140} that optimally describes, under the constraint of a representation in terms of apparent surface charges, the influence of solute charge that penetrates outside the cavity. Vertical excitation is treated by a nonequilibrium approach,^{134,141,142} with static and optical dielectric constants for water taken as 78.4 and 1.78, respectively. The implementation in QChem5 describes the cavity as the union of all atomic spheres with van der Waals radii multiplied by a factor of 1.2, and provides a switching/Gaussian (SWIG) blurring of the cavity surface charge density.¹⁴³⁻¹⁴⁵

Benchmark EOM-CCSD/aug-cc-pVDZ results were obtained for the five lowest excited states of each of the twenty clusters. Prior expectation is that the spectrum in the experimentally probed range will arise from excitations of the $3p$ electrons of Cl^- , which are degenerate in the gas phase and can be anticipated to lie close together in the somewhat asymmetric aqueous phase. The three lowest excited states in all the clusters were indeed verified to qualitatively correspond to holes in the $3p$ shell of Cl^- and to excited s -like electrons having centers near Cl^- , albeit with some minor delocalization of the holes and more extensive delocalization of the excited electrons onto nearby water, as expected for CTTS transitions. In each cluster the three lowest excited states are closely spaced within ≤ 0.19 eV, followed by a significant break ≥ 0.24 eV before the next higher ones appear. The different clusters however, show significant dispersion in their three lowest excitation energies, varying over a substantial energy range of 6.7-7.4 eV and oscillator strengths of 0.04-0.14.

For the five clusters containing only 5 water molecules each it was also feasible to carry out EOM-CCSD calculations with the larger aug-cc-pVTZ basis set^{132,133} and the same dielectric con-

tinuum treatment. Compared to the lowest three states of the same five clusters with EOM-CCSD/aug-cc-pVDZ these uniformly give only slightly higher excitation energies, by an average of 0.079 eV, and oscillator strengths very slightly larger by an average of only 0.002. It is concluded that the aug-cc-pVDZ basis set is quite adequate for EOM-CCSD benchmark calculations.

QM Protocol

To establish a more efficient protocol for feasible application to a much larger number of clusters, the twenty benchmark structures were also treated with eight different methods based on time-dependent density functional theory (TDDFT) that have been touted in the literature as being effective for excited state calculations. The base DFTs are known as PBE0,¹⁴⁶ CAM-B3LYP,¹⁴⁷ BMK,¹⁴⁸ MPWB1K,¹⁴⁹ ω B97X-D,¹⁵⁰ M062X,¹⁵¹ M11,¹⁵² and MN15.¹⁵³ Each of these was tested together with the 6-311++G**^{154,155} and the apcseg-1¹⁵⁶⁻¹⁵⁸ basis sets, both of which contain polarization and diffuse functions on all atoms, as well as the same dielectric continuum treatment described above.

The mean unsigned error (MUE) and mean signed error (MSE) of the TDDFT excitation energies E and oscillator strengths f , relative to the benchmark EOM-CCSD/aug-cc-pVDZ calculations, averaged over the lowest three transitions of all twenty selected clusters, are reported for each TDDFT/basis combination in Table 4, with the exception of MPWB1K/apcseg-1 which experienced severe convergence difficulties with almost all the clusters. Note that the errors are generally much smaller than the actual vertical excitation energies that range from 6.2-7.5 eV and oscillator strengths that range from 0.04-0.14.

Table 4 Average errors of TDDFT relative to benchmark EOM-CCSD/aug-cc-pVDZ calculations on the lowest three vertical excited state energies E in eV and oscillator strengths f for 20 selected clusters of chloride ion with water.

functional	basis set	E MUE(MSE)	f MUE(MSE)
PBE0	6-311++G**	0.700 (-0.700)	0.007 (-0.003)
CAM-B3LYP	6-311++G**	0.381 (-0.381)	0.012 (0.011)
BMK	6-311++G**	0.081 (0.081)	0.038 (0.037)
MPWB1K	6-311++G**	0.273 (-0.273)	0.013 (0.012)
ω B97X-D	6-311++G**	0.162 (-0.162)	0.029 (0.028)
M062X	6-311++G**	0.372 (-0.372)	0.011 (0.009)
M11	6-311++G**	0.349 (-0.349)	0.012 (-0.012)
MN15	6-311++G**	0.131 (-0.131)	0.047 (0.047)
PBE0	apcseg-1	0.756 (-0.756)	0.011 (-0.010)
CAM-B3LYP	apcseg-1	0.434 (-0.434)	0.006 (0.004)
BMK	apcseg-1	0.041 (0.039)	0.019 (0.019)
MPWB1K	apcseg-1	-	-
ω B97X-D	apcseg-1	0.205 (-0.205)	0.021 (0.021)
M062X	apcseg-1	0.425 (-0.425)	0.007 (-0.003)
M11	apcseg-1	0.420 (-0.420)	0.026 (-0.026)
MN15	apcseg-1	0.165 (-0.165)	0.043 (0.042)

Most of the DFT methods tested give energy MUE and MSE of several tenths of an eV compared to the benchmarks, and similar errors are obtained for the only case of MPWB1K/asegpc-1 that succeeded in converging. Somewhat better performance for energy MUE and MSE \lesssim 0.20 eV is seen with BMK, ω B97X-D, and MN15 for both the 6-311++G** and the apcseg-1 basis sets. The top performing method overall is BMK/apcseg-1, with energy

MUE and MSE of only 0.041 and 0.039 eV and oscillator strength MUE and MSE of 0.019. For the five cases of 5-coordination where comparison can be made, BMK/apcseg-1 agrees even better with the EOM-CCSD/aug-cc-pVTZ results (0.020, -0.019, 0.016, 0.014 for energy MUE, MSE in eV and oscillator strength MUE, MSE, respectively) than with the EOM-CCSD/aug-cc-pVDZ results (0.060, 0.060, 0.017, 0.016 for energy MUE, MSE in eV and oscillator strength MUE, MSE, respectively). Based on its excellent performance for the benchmarks, BMK/apcseg-1 was chosen as the QM protocol to be applied to a much larger selection of clusters.

To test whether a single shell of explicit water molecules is enough, a second shell of solvent was included in the twenty selected clusters by choosing all water molecules having O-Cl⁻ distances up to the second minimum of the corresponding RDF, together with the same dielectric continuum treatment described above outside of that. This produced clusters having anywhere from 19-33 explicit water molecules. Enlarging the clusters in this way changed the three lowest BMK/apcseg-1 excitation energies of the twenty clusters by MUE of only 0.084 eV, slightly raising them in nearly all cases, and changed the oscillator strengths by an unsigned average of only 0.014. It is concluded that surrounding Cl⁻ with just one shell of explicit solvent plus a dielectric continuum is quite adequate for the present study.

QM Results for Cl⁻ in Water

To treat the CTTS spectrum, selection at 20 ps intervals from the Cl⁻ MD simulation produced 5000 largely uncorrelated snapshots. Clusters containing Cl⁻ and all its first-shell water molecules with dielectric continuum outside that were extracted from the snapshots and subjected to BMK/apcseg-1 calculations on the five lowest excited states. It transpires that in the vast majority of cases only the three lowest excited states of the clusters contribute to the energy region of interest up to 7.5 eV, as expected. Only in 1.4% of cases does the fourth excited state contribute, and in no case does the fifth excited state contribute there. Thus, a quite sufficient number of excited states for each structure was included for the present purposes.

While different population analysis methods can give disparate quantitative results, such approaches can be useful to provide qualitative information. A previous MD simulation on aqueous Cl⁻⁵⁰ based on an earlier version of the AMOEBA force field found in QM calculations on extracted clusters that there is some charge transfer from the ion to solvent even in the ground state, obtaining an average Cl⁻ charge of -0.7 e from CHelpG¹⁵⁹ analysis or -0.8 e from QTAIM¹⁶⁰ theory. This CHelpG result is confirmed in the present QM calculations on 5000 snapshots, which find the average Cl⁻ charge (and its standard deviation) to be -0.70 (0.08) e . It is concluded that there is a significant amount of charge transfer from ground state Cl⁻ to water, with a distribution possibly ranging up to several tenths of an electron.

The difference between the excited and ground state electron density matrix provides considerable insight into the nature of a transition. Descriptors for each such density difference averaged over all transitions up to 7.5 eV are shown in Table 5.

Table 5 Descriptors of the excited to ground state density differences of aqueous Cl^- snapshots, given as average value in Å followed by standard deviation in parentheses. Listed are the distances of the hole and excited electron centroids from Cl^- and the hole and excited electron RMS sizes for different numbers of snapshots and different numbers of explicit solvation shells

snapshots	5000	20	20
solvation shells	1	1	2
hole centroid	0.11 (0.16)	0.10 (0.05)	0.09 (0.05)
excited electron centroid	0.39 (0.42)	0.39 (0.11)	0.52 (0.19)
hole size	1.48 (0.09)	1.48 (0.09)	1.51 (0.10)
excited electron size	4.15 (0.12)	4.10 (0.07)	4.28 (0.17)

For the full set of 5000 snapshots the small average distances of the hole and excited electron centroids from the Cl^- nucleus confirms that the excitations emanate from Cl^- . The electrons and holes are therefore quite close together, the distribution of their separations peaking at only ~ 0.28 Å, and being essentially negligible beyond ~ 0.8 Å. The average hole RMS size further shows the holes to be well localized on Cl^- . Given that a water molecule can be qualitatively characterized as having partial positive charge on the hydrogen atoms and partial negative charge on the oxygen atom, any delocalization of negative charge from the chloride ion onto solvent will tend to concentrate more about the hydrogen atoms than about the oxygen atoms. The excited electron RMS size is almost exactly midway between the first two maxima of the O- Cl^- RDF, which in conjunction with its rather narrow standard deviation, indicates it to be mostly localized on the outermost hydrogens of the first shell water molecules and the innermost hydrogens of the second shell water molecules. Taken together, these descriptors confirm that the excitations being analyzed are in fact CTTS transitions of Cl^- to nearby surrounding water.

For the small set of 20 snapshots used in determination of the QM protocol, the average values seen in Table 5 with one explicit solvation shell are very close to those from the full set of 5000, albeit with generally somewhat smaller standard deviations. The small set therefore serves as a suitable proxy for the larger set, which allows for comparison to the values where two explicit solvation shells are included. As seen in Table 5, the latter values do not change enough from those with one explicit solvation shell to alter any conclusions reached for the full set of 5000 snapshots, thereby reinforcing the point already reached earlier above that one explicit solvation shell is adequate for present purposes.

The lowest excited state energies and oscillator strengths from all the clusters provide a spectrum of many sticks having various positions and heights. These sticks were placed into a series of 0.03 eV wide bins, that value chosen large enough to produce a generally smooth overall envelope while still being a factor of 20 smaller than the width of the overall envelope, ensuring that the envelope is not sensitive to the precise value chosen for the bin width. The bin heights were each taken to be proportional to the sum of all the oscillator strengths of the states contained in the bin, and fitted for display by spline smoothing. While the molar absorption coefficient is proportional to oscillator strength, the proportionality constant is not known. The height of the cal-

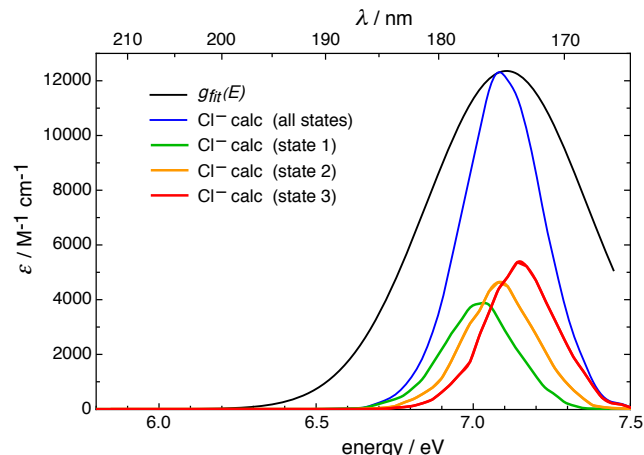


Fig. 5 Fitted experimental spectrum of aqueous Cl^- compared to the QM calculations on Cl^- in water.

culated spectrum envelope was therefore empirically scaled to match that of the fitted experimental spectrum. Hence, the calculated and experimental spectra can be meaningfully compared only in their positions and shapes, not their heights.

The calculated and fitted experimental spectra are shown in Fig. 5. The calculated spectrum is very nearly gaussian (correlation coefficient of fit $r^2 = 0.999$), like experiment. It peaks at 7.12 eV, in what is likely fortuitously excellent agreement with the peak at 7.106 eV in the fitted experimental spectrum. The shapes, however, are quite different, with the calculated spectrum about half as wide, having FWHM of 0.305 eV compared to 0.601 eV for the fitted experimental spectrum.

The contributions from each of the three subbands are also shown in Fig. 5. Each subband is nearly gaussian ($r^2 \geq 0.997$), with almost evenly-spaced peaks at 7.05, 7.12, and 7.18 eV and essentially equal FWHMs of 0.275, 0.274, and 0.274 eV, respectively. The peak heights are slightly different, such that the three subbands account for 28%, 33%, and 39% of the total area, respectively. Thus, the overall band envelope has significant contributions arising both from the separations of the subbands and from their individual widths.

It may be that the three quasi-degenerate $3p$ states of Cl^- interchange among one another faster than the solvent orientational dynamics, which would lead to a single excitation band instead of three separate overlapping subbands. This possibility of homogeneous broadening was raised, although not found, in a computational study of the hydrated electron¹⁶¹ that involves the analogous but reversed situation of an s -like ground state being excited into three quasidegenerate p -like excited states. Subsequent polarized transient hole-burning experiments concluded that the solvated electron spectrum in both water and methanol is indeed predominantly homogeneously broadened.¹⁶² The present calculations cannot properly address this notion for aqueous Cl^- . However, even it were happening it would not explain the discrepancy with experiment, since it would lead to narrowing of the calculated spectrum, making the disagreement with experiment even worse.

It is germane to estimate the otherwise absent effects of chlo-

rine spin-orbit coupling on the computational results to better compare with the experimental results that correspond to an unresolved mixture of the two spin-orbit doublet states. Given the small magnitude of the chlorine spin-orbit splitting of only 0.109 eV, this can be approximately done by superimposing two shifted copies of the computed spectrum, separating them by the experimental splitting. This produces a net spectrum that is still essentially Gaussian ($r^2=0.9997$) with FWHM of 0.334 eV. That value is only slightly larger than the computed FWHM of 0.305 eV obtained without consideration of spin-orbit splitting, and is still much smaller than the experimental FWHM of 0.601 eV. It is concluded that spin-orbit coupling can account for only a small part of the discrepancy with experiment on the spectral width.

In a search for possible associations it was determined that there is no significant correlation ($r^2 < 0.10$) of the calculated excitation energies with the MD coordination number of Cl^- or with its QM-determined ground state charge.

It can be noted that an analogous strategy of carrying out MD simulations to provide snapshots for QM analysis gave an adequate description of both the position and band width observed for the lower component of the spin-orbit doublet in the CTTS spectrum of aqueous iodide I^- .²² Be that as it may, the spin-orbit components of the I^- spectrum are only about half as wide as in the Cl^- spectrum,⁶ so possibly making it an easier target to match.

QM Results for NaCl in Water

To investigate the possible influence of ion pairing on the CTTS spectrum, selection at 20 ps intervals from the NaCl MD simulation produced 15000 largely uncorrelated snapshots. From these were included all 419 instances of the CIP, all 2581 instances of the SIP, all 3025 instances of the 2SIP, and 5000 of the 8975 instances of the Free categories. In each of the four categories the clusters extracted from the snapshots included Cl^- and all waters within its first solvation shell. With the CIP and SIP categories, Na^+ and all waters within its first solvation shell were also included. With the 2SIP and Free categories the $\text{Na}^+\text{-Cl}^-$ separation is larger than the first solvation shell of Cl^- , so no counterion or associated waters were included in those cases, although their influence is still felt in how they affect the solvation shell around Cl^- .

TDDFT calculations were carried out on all of these clusters, again using the BMK/apcseg-1 method with dielectric continuum. The stick spectra were binned, fitted, and the height scaled in the same way as described above for the Cl^- spectra, producing the aqueous NaCl spectrum shown in Fig. 6. The spectrum is nearly gaussian ($r^2 = 0.998$) with peak at 7.06 eV and FWHM of 0.280 eV. These values are only slightly smaller than the 7.12 eV peak and 0.305 eV FWHM found for the Cl^- spectrum obtained without the counterion. It is concluded that the counterion has only a minor influence on the calculated spectrum.

Individual contributions to the spectrum from the CIP, SIP, 2SIP, and Free categories are also shown in Fig. 6. Note that the much fewer instances of CIP makes that category subject to considerably more statistical uncertainty than for the other cate-

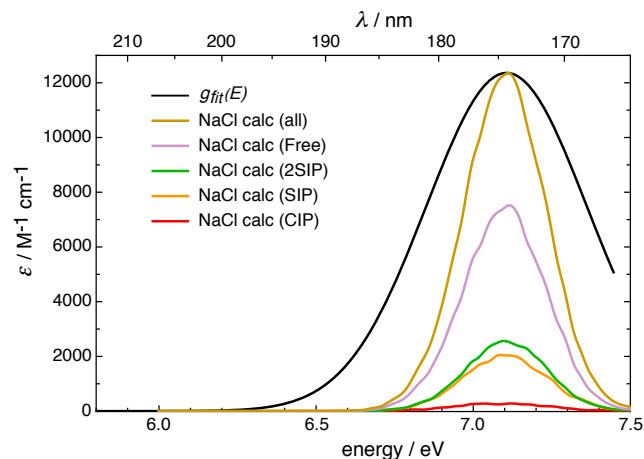


Fig. 6 Fitted experimental spectrum of aqueous Cl^- compared to the QM calculations on NaCl in water.

gories. The spectrum for each of the categories is nearly gaussian ($r^2 = 0.979, 0.995, 0.993, \text{ and } 0.999$, respectively). The almost equal peaks of 7.04, 7.06, 7.06, and 7.05 eV, respectively, differ only slightly from the peak of the overall spectrum at 7.06 eV, and the almost equal FWHMs of 0.287, 0.284, 0.271, and 0.283 eV, respectively, differ only slightly from the FWHM of the overall spectrum of 0.280 eV. It is concluded that each category of ion pairing gives very nearly the same computed spectrum as the other categories and nearly the same spectrum as that obtained without counterions.

CONCLUDING DISCUSSION

One interesting and surprising takeaway from this work is that ionic strength does not affect the aqueous Cl^- CTTS spectrum up to at least 0.25 M salt concentration, as clearly established experimentally and also found in the computations. To learn more about this we plan future experimental work to systematically investigate the effect of ionic strength on the CTTS transitions over a broad range of concentrations, temperatures, and counterions.

It is also puzzling that the elaborate QM computations made here give a width of the Cl^- CTTS only about half that of experiment even while providing excellent agreement with experiment on the peak position. It is then most likely that the qualitative discrepancy between the computed and experimental spectral widths lies in a failure of the underlying MD simulations to provide an appropriate variety of structures. There is no apparent explanation for the source of this inadequacy. For example, the RDFs obtained from the MD simulations agree well with experiment for Cl^- and Na^+ , and also, as far as can be discerned, for NaCl as well. Also, there is no significant correlation of the calculated excitation energies with the MD coordination number of Cl^- or with its distance to the nearest water molecule or sodium ion, nor is there with its QM-determined ground state charge. A couple of speculations on other possible sources of the problem can be offered.

One possibility is that partial charge transfer of up to several tenths of an electron from ground state Cl^- to water molecules, such as is suggested in the QM results by qualitative population

analysis schemes, might significantly modify the distribution of MD structures and so alter the QM excitation energies a sufficient amount to provide the necessary width of the spectrum. Indeed, analogous additional MD and subsequent QM calculations not otherwise presented here obtained with MD charges on Cl^- of -0.9 , -0.8 , and $-0.7 e$, albeit without taking into account in the MD the missing total charge, indicate that these calculated spectra have nearly the same width as that obtained with the full Cl^- charge throughout but have peak positions shifted to lower energy by ~ 0.12 eV for each change in the Cl^- charge by $0.1 e$. Considering the net spectrum as some linear combination of these separate spectra would be sufficient to form a full spectral width in agreement with experiment, at the sacrifice of only a small deterioration of the excellent agreement with experiment on the peak position. But consideration of the solvation energy strongly argues against this explanation. The solvation free energy of a spherical ion can be qualitatively analyzed in terms of the simple Born model expression given by $\Delta G_{\text{Born}} = -(\epsilon - 1)q^2 / (2\epsilon R)$ with ϵ the static dielectric constant of the solvent, q the ion charge, and R the radius of the cavity containing the solute ion.¹⁶³ The dominant effect in this expression from a small change in the Cl^- charge would be in the factor q^2 , while any attendant change in R should be only a secondary effect. The dependence on the square of q indicates that any significant ground state charge transfer to solvent would have a huge effect on the Cl^- solvation energy, thereby spoiling the otherwise good agreement with experiment calculated for this property.²⁶

Another possibility is based on time scales. The fact that the AMOEBA force field provides reasonable accounts of several disparate experimental results, including the Cl^- solvation energy²⁶ and, as shown here, the Cl^- to water RDFs and QM determination of the Cl^- UV spectrum peak position, indicates that the MD simulation reliably provides structures representative of time-averaged solvent. However, unlike those properties, vertical excitation occurs on a much shorter time scale than solvent fluctuations. The width of the UV spectrum might be particularly sensitive to a wide variety of instantaneous solvent configurations that differ significantly from the time-average, and that class of configurations may not be adequately sampled in the MD simulation.

Should either of these possibilities be the case, the problem encountered in this work would likely be present more universally in classical MD simulations of many other aqueous anions than just to the situation of Cl^- explored here.

Whatever the reason, it is evident that the high quality classical MD simulation used in this study fails to provide an adequate variety of structures to allow for QM rationalization of the width of the experimental aqueous Cl^- spectrum. Further work is clearly warranted to establish a clarification of the deficiency. It would be interesting to see if the state of the art in either QM/MM, which for example has proven useful to obtain structures for spectroscopic calculations on the aqueous OH radical,^{164,165} or in full AIMD can solve this problem.

CONFLICTS OF INTEREST

There are no conflicts of interest to declare.

ACKNOWLEDGEMENTS

The research described herein was supported by the Division of Chemical Sciences, Geosciences and Biosciences, Basic Energy Sciences, Office of Science, United States Department of Energy through grant number DE-FC02-04ER15533. This is contribution number NDRL-5310 from the Notre Dame Radiation Laboratory. Helpful discussions were made with Dr. Benjamin Schwartz.

Notes and references

- 1 M. Smith and M. C. R. Symons, *Trans. Faraday Soc.*, 1958, **54**, 338–345.
- 2 J. Jortner, M. Ottolenghi and G. Stein, *J. Phys. Chem.*, 1964, **68**, 247–255.
- 3 M. J. Blandamer and M. F. Fox, *Chem. Rev.*, 1970, **70**, 59–93.
- 4 E. Rabinowitch, *Rev. Mod. Phys.*, 1942, **14**, 112–131.
- 5 M. F. Fox, B. E. Barker and E. Hayon, *J. C. S. Faraday Trans. I*, 1978, **74**, 1776–1785.
- 6 T. W. Marin, I. Janik and D. M. Bartels, *Phys. Chem. Chem. Phys.*, 2019, **21**, 24419–24428.
- 7 J. W. Spinks and R. J. Woods, *An Introduction to Radiation Chemistry*, J. Wiley and Sons: New York, 3rd edn, 1990.
- 8 G. V. Buxton, C. L. Greenstock, W. P. Helman and A. B. Ross, *J. Phys. Chem. Ref. Data*, 1988, **17**, 513–886.
- 9 B. C. Garrett, D. A. Dixon, D. M. Camaioni, D. M. Chipman, M. A. Johnson, C. D. Jonah, G. A. Kimmel, J. H. Miller, T. N. Rescigno, P. J. Rossky, S. S. Xantheas, S. D. Colson, A. H. Laufer, D. Ray, P. F. Barbara, D. M. Bartels, K. H. Becker, H. Bowen, S. E. Bradforth, I. Carmichael, J. V. Coe, L. R. Corrales, J. P. Cowin, M. Dupuis, K. B. Eisenthal, J. A. Franz, M. S. Gutowski, K. D. Jordan, B. D. Kay, J. A. LaVerne, S. V. Lymar, T. E. Madey, C. W. McCurdy, D. Meisel, S. Mukamel, A. R. Nilsson, T. M. Orlando, N. G. Petrik, S. M. Pimblott, J. R. Rustad, G. K. Schenter, S. J. Singer, A. Tokmakoff, L. S. Wang, C. Wittig and T. S. Zwier, *Chem. Rev.*, 2005, **105**, 355–389.
- 10 D. Majumdar, J. Kim and K. S. Kim, *J. Chem. Phys.*, 2000, **112**, 101–105.
- 11 J. Kim, H. M. Lee, S. B. Suh, D. Majumdar and K. S. Kim, *J. Chem. Phys.*, 2000, **113**, 5259–5272.
- 12 H. M. Lee, D. Kim and K. S. Kim, *J. Chem. Phys.*, 2002, **116**, 5509–5520.
- 13 M. Kolaski, H. Lee, C. Pak, A. Dupuis and K. Kim, *J. Phys. Chem. A*, 2005, **109**, 9419–9423.
- 14 W.-S. Sheu and Y.-T. Liu, *Chem. Phys. Lett.*, 2003, **374**, 620–625.
- 15 W.-S. Sheu and Y.-T. Liu, *Chem. Phys. Lett.*, 2004, **399**, 73–77.
- 16 D. Borgis and A. Staib, *Chem. Phys. Lett.*, 1994, **230**, 405–413.
- 17 A. Staib and D. Borgis, *J. Chem. Phys.*, 1995, **103**, 2642–2655.
- 18 D. Borgis and A. Staib, *J. Chem. Phys.*, 1996, **104**, 4776–4783.
- 19 A. Staib and D. Borgis, *J. Chem. Phys.*, 1996, **104**, 9027–

- 9039.
- 20 D. Borgis and A. Staib, *J. Phys. Cond. Mat.*, 1996, **8**, 9389–9395.
- 21 N. Galamba, R. A. Mata and B. J. Costa Cabral, *J. Phys. Chem. A*, 2009, **113**, 14684–14690.
- 22 S. Bradforth and P. Jungwirth, *J. Phys. Chem. A*, 2002, **106**, 1286–1298.
- 23 J. E. Sansonetti and W. C. Martin, *J. Phys. Chem. Ref. Data*, 2005, **34**, 1559–2259.
- 24 J. W. Ponder, *TINKER: Software Tools for Molecular Design, version 8.6*, <http://dasher.wustl.edu/tinker/>, Washington University in St. Louis, 2019.
- 25 J. A. Rackers, Z. Wang, C. Lu, M. L. Laury, L. Lagardère, M. J. Schnieders, J.-P. Piquemal, P. Ren and J. W. Ponder, *J. Chem. Theory Comp.*, 2018, **14**, 5273–5289.
- 26 M. L. Laury, L.-P. Wang, V. S. Pande, T. Head-Gordon and J. W. Ponder, *J. Phys. Chem. B*, 2015, **119**, 9423–9437.
- 27 S. Cummings, J. E. Enderby, G. W. Neilson, J. R. Newsome, R. A. Howe, W. S. Howells and A. K. Soper, *Nature*, 1980, **287**, 714–716.
- 28 H. J. C. Berendsen, J. P. M. Postma, W. F. van Gunsteren, A. Dinola and J. R. Haak, *J. Chem. Phys.*, 1984, **81**, 3684–3690.
- 29 T. Morishita, *J. Chem. Phys.*, 2000, **113**, 2976–2982.
- 30 D. Beeman, *J. Comp. Phys.*, 1976, **20**, 130–139.
- 31 B. R. Brooks, *National Institutes of Health: Bethesda, MD*, 1988.
- 32 P. C. Vogel and K. Heinzinger, *Z. Naturforsch.*, 1976, **31a**, 476–481.
- 33 R. W. Impey, P. A. Madden and I. R. McDonald, *J. Phys. Chem.*, 1983, **87**, 5071–5083.
- 34 J. P. Limtrakul and B. M. Rode, *Mon. Chem.*, 1985, **116**, 1377–1383.
- 35 A. C. Belch, M. Berkowitz and J. A. McCammon, *J. Am. Chem. Soc.*, 1986, **108**, 1755–1761.
- 36 M. Sprik, M. L. Klein and K. Watanabe, *J. Phys. Chem.*, 1990, **94**, 6483–6488.
- 37 L. X. Dang, J. E. Rice and P. A. Kollman, *J. Chem. Phys.*, 1990, **93**, 7528–7529.
- 38 L. X. Dang, J. E. Rice, J. Caldwell and P. A. Kollman, *J. Am. Chem. Soc.*, 1991, **113**, 2481–2486.
- 39 E. Guàrdia, R. Rey and J. A. Padró, *J. Chem. Phys.*, 1991, **95**, 2823–2831.
- 40 D. E. Smith and L. X. Dang, *J. Chem. Phys.*, 1994, **100**, 3757–3766.
- 41 G. Tóth, *J. Chem. Phys.*, 1996, **105**, 5518–5524.
- 42 E. Guàrdia and J. A. Padró, *Mol. Sim.*, 1996, **17**, 83–94.
- 43 S. Koneshan and J. C. Rasaiah, *J. Chem. Phys.*, 2000, **113**, 8125–8137.
- 44 S. Chowdhuri and A. Chandra, *J. Chem. Phys.*, 2001, **115**, 3732–3741.
- 45 L. X. Dang, *J. Phys. Chem. B*, 2002, **106**, 10388–10394.
- 46 L. X. Dang, G. K. Schenter, V.-A. Glezakou and J. L. Fulton, *J. Phys. Chem. B*, 2006, **110**, 23644–23654.
- 47 S. Bouazizi, S. Nasr, N. Jaïdane and M.-C. Bellissent-Funel, *J. Phys. Chem. B*, 2006, **110**, 23515–23523.
- 48 S. A. Hassan, *J. Phys. Chem. B*, 2008, **112**, 10573–10584.
- 49 M. B. Webb, S. H. Garofalini and G. W. Scherer, *J. Phys. Chem. B*, 2009, **113**, 9886–9893.
- 50 Z. Zhao, D. M. Rogers and T. L. Beck, *J. Chem. Phys.*, 2010, **132**, 014502:1–10.
- 51 D. M. Rogers and T. L. Beck, *J. Chem. Phys.*, 2010, **132**, 014505:1–12.
- 52 P. Gallo, D. Corradini and M. Rovere, *Phys. Chem. Chem. Phys.*, 2011, **13**, 19814–19822.
- 53 M. Trumm, Y. O. G. Martínez, F. Réal, M. Masella, V. Vallet and B. Schimmelpfennig, *J. Chem. Phys.*, 2012, **136**, 044509:1–9.
- 54 A. Ghaffari and A. Rahbar-Kelishami, *J. Mol. Liq.*, 2013, **187**, 238–245.
- 55 H. V. R. Annapureddy and L. X. Dang, *J. Phys. Chem. C*, 2014, **118**, 7886–7891.
- 56 H. Chen and E. Ruckenstein, *J. Phys. Chem. B*, 2015, **119**, 12671–12676.
- 57 S. Roy, M. D. Baer, C. J. Mundy and G. K. Schenter, *J. Phys. Chem. C*, 2016, **120**, 7597–7605.
- 58 M. Mezei and D. L. Beveridge, *J. Chem. Phys.*, 1981, **74**, 6902–6910.
- 59 J. Chandrasekhar, D. C. Spellmeyer and W. L. Jorgensen, *J. Am. Chem. Soc.*, 1984, **106**, 903–910.
- 60 J. Marti and F. S. Csajka, *J. Chem. Phys.*, 2000, **113**, 1154–1161.
- 61 E. Jardón-Valadez and M. E. Costas, *J. Mol. Struct.-Theochem*, 2004, **677**, 227–236.
- 62 K. P. Jensen and W. L. Jorgensen, *J. Chem. Theory Comp.*, 2006, **2**, 1499–1509.
- 63 B. M. Pettitt and P. J. Rossky, *J. Chem. Phys.*, 1986, **84**, 5836–5844.
- 64 P. G. Kusalik and G. N. Patey, *J. Chem. Phys.*, 1988, **88**, 7715–7738.
- 65 P. G. Kusalik and G. N. Patey, *J. Chem. Phys.*, 1988, **89**, 5843–5851.
- 66 G. Hummer and D. M. Soumpasis, *Mol. Phys.*, 1992, **75**, 633–651.
- 67 G. Hummer, D. M. Soumpasis and M. Neumann, *Mol. Phys.*, 1992, **77**, 769–785.
- 68 A. Kovalenko and T. N. Truong, *J. Chem. Phys.*, 2000, **113**, 7458–7470.
- 69 I. S. Joung, T. Luchko and D. A. Case, *J. Chem. Phys.*, 2013, **138**, 044103:1–15.
- 70 J. M. Heuft and E. J. Meijer, *J. Chem. Phys.*, 2003, **119**, 11788–11791.
- 71 A. Bankura, V. Carnevale and M. L. Klein, *J. Chem. Phys.*, 2013, **138**, 014501:1–10.
- 72 C. Zhang, T. A. Pham, F. Gygi and G. Galli, *J. Chem. Phys.*, 2013, **138**, 181102:1–4.
- 73 L. Ge, L. Bernasconi and P. Hunt, *Phys. Chem. Chem. Phys.*,

- 2013, **15**, 13169–13183.
- 74 A. P. Gaiduk, C. Zhang, F. Gygi and G. Galli, *Chem. Phys. Lett.*, 2014, **604**, 89–96.
- 75 A. Bankura, B. Santra, R. A. D. Jr., C. W. Swartz, M. L. Klein and X. Wu, *Mol. Phys.*, 2015, **113**, 2842–2854.
- 76 T. A. Pham, T. Ogitsu, E. Y. Lau and E. Schwegler, *J. Chem. Phys.*, 2016, **145**, 154501:1–9.
- 77 A. P. Gaiduk and G. Galli, *J. Phys. Chem. Lett.*, 2017, **8**, 1496–1502.
- 78 M. DelloStritto, J. Xu, X. Wu and M. L. Klein, *Phys. Chem. Chem. Phys.*, 2020, **22**, 10666–10675.
- 79 H. Ma, *Int. J. Quant. Chem.*, 2014, **114**, 1006–1011.
- 80 R. Mancinelli, A. Botti, F. Bruni, M. A. Ricci and A. K. Soper, *J. Phys. Chem. B*, 2007, **111**, 13570–13577.
- 81 M. Antalek, E. Pace, B. Hedman, K. O. Hodgson, G. Chillemi, M. Benfatto, R. Sarangi and P. Frank, *J. Chem. Phys.*, 2016, **145**, 044318:1–15.
- 82 Y. Kameda, Y. Amo, T. Usuki, Y. Umabayashi, K. Ikeda and T. Otomo, *Bull. Chem. Soc. Japan*, 2019, **92**, 754–767.
- 83 I. G. Tironi, R. Sperb, P. E. Smith and W. F. van Gunsteren, *J. Chem. Phys.*, 1995, **102**, 5451–5459.
- 84 K. Hermansson and M. Wojcik, *J. Phys. Chem. B*, 1998, **102**, 6089–6097.
- 85 L. X. Dang, G. K. Schenter and C. D. Wick, *J. Phys. Chem. C*, 2017, **121**, 10018–10026.
- 86 P. G. Kusalik and G. N. Patey, *J. Chem. Phys.*, 1990, **92**, 1345–1358.
- 87 Y. Marcus and G. Hefter, *Chem. Rev.*, 2006, **106**, 4585–4621.
- 88 J.-J. Max, V. Gessinger, C. van Driessche, P. Larouche and C. Chapados, *J. Chem. Phys.*, 2007, **126**, 184507:1–14.
- 89 M. Berkowitz, O. A. Karim, J. McCammon and P. J. Rossky, *Chem. Phys. Lett.*, 1984, **105**, 577–580.
- 90 O. A. Karim and J. A. McCammon, *J. Am. Chem. Soc.*, 1986, **108**, 1762–1766.
- 91 J. Van Eerden, W. Briels, S. Harkema and D. Feil, *Chem. Phys. Lett.*, 1989, **164**, 370 – 376.
- 92 E. Guàrdia, R. Rey and J. Padró, *Chem Phys.*, 1991, **155**, 187–195.
- 93 L. X. Dang, *J. Chem. Phys.*, 1992, **97**, 1919–1921.
- 94 H. Resat, M. Mezei and J. A. McCammon, *J. Phys. Chem.*, 1996, **100**, 1426–1433.
- 95 A. P. Lyubartsev and A. Laaksonen, *J. Phys. Chem.*, 1996, **100**, 16410–16418.
- 96 P. L. Geissler, C. Dellago and D. Chandler, *J. Phys. Chem. B*, 1999, **103**, 3706–3710.
- 97 L. Degrève and F. L. B. da Silva, *J. Chem. Phys.*, 1999, **111**, 5150–5156.
- 98 L. Degrève and F. L. B. da Silva, *J. Mol. Liq.*, 2000, **87**, 217–232.
- 99 H. Uchida and M. Matsuoka, *Fluid Phase Equil.*, 2004, **219**, 49–54.
- 100 A. A. Chen and R. V. Pappu, *J. Phys. Chem. B*, 2007, **111**, 6469–6478.
- 101 I. V. Khavrutskii, J. Dzubiella and J. A. McCammon, *J. Chem. Phys.*, 2008, **128**, 044106:1–13.
- 102 A. Savelyev and G. A. Papoian, *J. Phys. Chem. B*, 2009, **113**, 7785–7793.
- 103 C. D. Wick and L. X. Dang, *J. Chem. Phys.*, 2010, **132**, 044702:1–8.
- 104 J. Timko, D. Bucher and S. Kuyucak, *J. Chem. Phys.*, 2010, **132**, 114510:1–8.
- 105 K. Yui, M. Sakuma and T. Funazukuri, *Fluid Phase Equil.*, 2010, **297**, 227–235.
- 106 A. Mirzoev and A. P. Lyubartsev, *Phys. Chem. Chem. Phys.*, 2011, **13**, 5722–5727.
- 107 Y. Luo, W. Jiang, H. Yu, A. D. MacKerell and B. Roux, *Faraday Discuss.*, 2013, **160**, 135–149.
- 108 S. Keshri, A. Sarkar and B. L. Tembe, *J. Phys. Chem. B*, 2015, **119**, 15471–15484.
- 109 M. Kelley, A. Donley, S. Clark and A. Clark, *J. Phys. Chem. B*, 2015, **119**, 15652–15661.
- 110 M. Soniat, G. Pool, L. Franklin and S. W. Rick, *Fluid Phase Equil.*, 2016, **407**, 31–38.
- 111 C. Wang, P. Ren and R. Luo, *J. Phys. Chem. B*, 2017, **121**, 11169–11179.
- 112 T. J. Yoon, L. A. Patel, M. J. Vigil, K. A. Maerzke, A. T. Findikoglu and R. P. Currier, *J. Chem. Phys.*, 2019, **151**, 224504:1–10.
- 113 P. G. Kusalik and G. N. Patey, *J. Chem. Phys.*, 1988, **89**, 7478–7484.
- 114 J. Perkyns and B. M. Pettitt, *Chem. Phys. Lett.*, 1992, **190**, 626–630.
- 115 G. Hummer, D. M. Soumpasis and M. Neumann, *Mol. Phys.*, 1994, **81**, 1155–1163.
- 116 A. Kovalenko and F. Hirata, *J. Chem. Phys.*, 2000, **112**, 10391–10402.
- 117 A. Kovalenko and F. Hirata, *J. Chem. Phys.*, 2000, **112**, 10403–10417.
- 118 M. Kinoshita and Y. Harano, *Bull. Chem. Soc. Japan*, 2005, **78**, 1431–1441.
- 119 A. A. Rashin, *J. Phys. Chem.*, 1989, **93**, 4664–4669.
- 120 L. R. Pratt, G. Hummer and A. E. Garcia', *Biophys. Chem.*, 1994, **51**, 147–165.
- 121 J. Trullàs, A. Giró and J. A. Padró, *J. Chem. Phys.*, 1989, **91**, 539–545.
- 122 J. Trullàs, A. Giró and J. A. Padró, *J. Chem. Phys.*, 1990, **93**, 5177–5181.
- 123 J. A. Padró, J. Trullàs and A. Giró, *J. Chem. Soc. Faraday Trans.*, 1990, **86**, 2139–2143.
- 124 M. Canales and G. Sesé, *J. Chem. Phys.*, 1998, **109**, 6004–6011.
- 125 J. Gujt, M. Bešter-Rogač and B. Hribar-Lee, *J. Mol. Liq.*, 2014, **190**, 34–41.
- 126 R. A. Friedman and M. Mezei, *J. Chem. Phys.*, 1995, **102**, 419–426.
- 127 Y. Yao and Y. Kanai, *J. Chem. Theory Comp.*, 2018, **14**, 884–893.

- 128 D. A. McQuarrie, *Statistical Mechanics*, University Science Books, Sausalito, CA, 2000.
- 129 Y. Shao, Z. Gan, E. Epifanovsky, A. T. Gilbert, M. Wormit, J. Kussmann, A. W. Lange, A. Behn, J. Deng, X. Feng, D. Ghosh, M. Goldey, P. R. Horn, L. D. Jacobson, I. Kaliman, R. Z. Khaliullin, T. Kuš, A. Landau, J. Liu, E. I. Proynov, Y. M. Rhee, R. M. Richard, M. A. Rohrdanz, R. P. Steele, E. J. Sundstrom, H. L. W. III, P. M. Zimmerman, D. Zuev, B. Albrecht, E. Alguire, B. Austin, G. J. O. Beran, Y. A. Bernard, E. Berquist, K. Brandhorst, K. B. Bravaya, S. T. Brown, D. Casanova, C.-M. Chang, Y. Chen, S. H. Chien, K. D. Closser, D. L. Crittenden, M. Diedenhofen, R. A. D. Jr., H. Do, A. D. Dutoi, R. G. Edgar, S. Fatehi, L. Fusti-Molnar, A. Ghysels, A. Golubeva-Zadorozhnaya, J. Gomes, M. W. Hanson-Heine, P. H. Harbach, A. W. Hauser, E. G. Hohenstein, Z. C. Holden, T.-C. Jagau, H. Ji, B. Kaduk, K. Khistyayev, J. Kim, J. Kim, R. A. King, P. Klunzinger, D. Kosenkov, T. Kowalczyk, C. M. Krauter, K. U. Lao, A. D. Laurent, K. V. Lawler, S. V. Levchenko, C. Y. Lin, F. Liu, E. Livshits, R. C. Lochan, A. Luenser, P. Manohar, S. F. Manzer, S.-P. Mao, N. Mardirossian, A. V. Marenich, S. A. Maurer, N. J. Mayhall, E. Neuscammann, C. M. Oana, R. Olivares-Amaya, D. P. O'Neill, J. A. Parkhill, T. M. Perrine, R. Peverati, A. Prociuk, D. R. Rehn, E. Rosta, N. J. Russ, S. M. Sharada, S. Sharma, D. W. Small, A. Sodt, T. Stein, D. Stück, Y.-C. Su, A. J. Thom, T. Tsuchimochi, V. Vanovschi, L. Vogt, O. Vydrov, T. Wang, M. A. Watson, J. Wenzel, A. White, C. F. Williams, J. Yang, S. Yeganeh, S. R. Yost, Z.-Q. You, I. Y. Zhang, X. Zhang, Y. Zhao, B. R. Brooks, G. K. Chan, D. M. Chipman, C. J. Cramer, W. A. G. III, M. S. Gordon, W. J. Hehre, A. Klamt, H. F. S. III, M. W. Schmidt, C. D. Sherrill, D. G. Truhlar, A. Warshel, X. Xu, A. Aspuru-Guzik, R. Baer, A. T. Bell, N. A. Besley, J.-D. Chai, A. Dreuw, B. D. Dunietz, T. R. Furlani, S. R. Gwaltney, C.-P. Hsu, Y. Jung, J. Kong, D. S. Lambrecht, W. Liang, C. Ochsenfeld, V. A. Rassolov, L. V. Slipchenko, J. E. Subotnik, T. V. Voorhis, J. M. Herbert, A. I. Krylov, P. M. Gill and M. Head-Gordon, *Mol. Phys.*, 2015, **113**, 184–215.
- 130 E. Dalgaard and H. J. Monkhorst, *Phys. Rev. A*, 1983, **28**, 1217–1222.
- 131 H. Sekino and R. J. Bartlett, *Intern. J. Quantum. Chem.*, 1984, **26**, 255–265.
- 132 T. H. Dunning, *J. Chem. Phys.*, 1989, **90**, 1007–1023.
- 133 R. A. Kendall, T. H. Dunning and R. J. Harrison, *J. Chem. Phys.*, 1992, **96**, 6796–6806.
- 134 J. Tomasi, B. Mennucci and R. Cammi, *Chem. Rev.*, 2005, **105**, 2999–3094.
- 135 A. Klamt and G. Schüürmann, *J. Chem. Soc., Perkin Trans. 2*, 1993, 799–805.
- 136 T. N. Truong and E. V. Stefanovich, *Chem. Phys. Lett.*, 1995, **240**, 253–260.
- 137 V. Barone and M. Cossi, *J. Phys. Chem. A*, 1998, **102**, 1995–2001.
- 138 B. Mennucci, R. Cammi and J. Tomasi, *J. Chem. Phys.*, 1998, **109**, 2798–2807.
- 139 D. M. Chipman, *J. Chem. Phys.*, 2000, **112**, 5558–5565.
- 140 D. M. Chipman, *Theor. Chem. Acc.*, 2002, **107**, 80–89.
- 141 D. M. Chipman, *J. Chem. Phys.*, 2009, **131**, 014103:1–6.
- 142 J.-M. Mewes, Z.-Q. You, M. Wormit, T. Kriesche, J. M. Herbert and A. Dreuw, *J. Phys. Chem. A*, 2015, **119**, 5446–5464.
- 143 D. M. York and M. Karplus, *J. Phys. Chem. A*, 1999, **103**, 11060–11079.
- 144 A. W. Lange and J. M. Herbert, *J. Phys. Chem. Lett.*, 2010, **1**, 556–561.
- 145 A. W. Lange and J. M. Herbert, *J. Chem. Phys.*, 2010, **133**, 244111:1–18.
- 146 C. Adamo and V. Barone, *J. Chem. Phys.*, 1999, **110**, 6158–6170.
- 147 T. Yanai, D. P. Tew and N. C. Handy, *Chem. Phys. Lett.*, 2004, **393**, 51–57.
- 148 A. D. Boese and J. M. L. Martin, *J. Chem. Phys.*, 2004, **121**, 3405–3416.
- 149 Y. Zhao and D. G. Truhlar, *J. Phys. Chem. A*, 2004, **108**, 6908–6918.
- 150 J.-D. Chai and M. Head-Gordon, *Phys. Chem. Chem. Phys.*, 2008, **10**, 6615–6620.
- 151 Y. Zhao and D. G. Truhlar, *Theor. Chem. Acc.*, 2008, **120**, 215–241.
- 152 R. Peverati and D. G. Truhlar, *J. Phys. Chem. Lett.*, 2011, **2**, 2810–2817.
- 153 H. S. Yu, X. He, S. L. Li and D. G. Truhlar, *Chem. Sci.*, 2016, **7**, 5032–5051.
- 154 R. Krishnan, J. S. Binkley, R. Seeger and J. A. Pople, *J. Chem. Phys.*, 1980, **72**, 650–654.
- 155 T. Clark, J. Chandrasekhar, G. W. Spitznagel and P. V. R. Schleyer, *J. Comp. Chem.*, 1983, **4**, 294–301.
- 156 F. Jensen, *J. Chem. Phys.*, 2001, **115**, 9113–9125.
- 157 F. Jensen, *J. Chem. Phys.*, 2002, **116**, 7372–7379.
- 158 F. Jensen, *J. Chem. Phys.*, 2002, **117**, 9234–9240.
- 159 C. M. Breneman and K. B. Wiberg, *J. Comp. Chem.*, 1990, **11**, 361–373.
- 160 R. F. W. Bader, *Atoms in Molecules: A Quantum Theory*, Clarendon, Oxford, 1990.
- 161 B. Schwartz and P. Rossky, *Phys. Rev. Lett.*, 1994, **72**, 3282–3285.
- 162 M. Cavanagh, I. Martini and B. Schwartz, *Chem. Phys. Lett.*, 2004, **396**, 359–366.
- 163 M. Born, *Zeit. für Physik*, 1920, **1**, 45–48.
- 164 L. Kjellsson, K. D. Nanda, J.-E. Rubensson, G. Doumy, S. H. Southworth, P. J. Ho, A. M. March, A. Al Haddad, Y. Kumagai, M.-F. Tu, R. D. Schaller, T. Debnath, M. S. B. M. Yusof, C. Arnold, W. F. Schlotter, S. Moeller, G. Coslovich, J. D. Koralek, M. P. Minitti, M. L. Vidal, M. Simon, R. Santra, Z.-H. Loh, S. Coriani, A. Krylov, I and L. Young, *Phys. Rev. Lett.*, 2020, **124**, 236001:1–7.
- 165 B. Rana and J. M. Herbert, *Phys. Chem. Chem. Phys.*, 2020, **22**, 27829–27844.